Li et al. Nanoscale Research Letters (2017) 12:576
DOI 10.1186/s11671-017-2342-z

Nanoscale Research Letters

NANO EXPRESS Open Access

Synthesis of Spherical Silver-coated $Li_4Ti_5O_{12}$ Anode Material by a Sol-Gel-assisted Hydrothermal Method

Jun Li*, Si Huang, Shuaijun Xu, Lifang Lan, Lu Lu and Shaofang Li

Abstract

Ag-coated spherical $Li_4Ti_5O_{12}$ composite was successfully synthesized via a sol-gel-assisted hydrothermal method using an ethylene glycol and silver nitrate mixture as the precursor, and the influence of the Ag coating contents on the electrochemical properties of its was extensively investigated. X-ray diffraction (XRD) analysis indicated that the Ag coating does not change the spinel structure of $Li_4Ti_5O_{12}$. The electrochemical impedance spectroscopy (EIS) analyses demonstrated that the excellent electrical conductivity of the $Li_4Ti_5O_{12}$/Ag resulted from the presence of the highly conducting silver coating layer. Additionally, the nano-thick silver layer, which was uniformly coated on the particles, significantly improved this material's rate capability. As a consequence, the silver-coated micron-sized spherial $Li_4Ti_5O_{12}$ exhibited excellent electrochemical performance. Thus, with an appropriate silver content of 5 wt.%, the $Li_4Ti_5O_{12}$/Ag delivered the highest capacity of 186.34 mAh g^{-1} at 0.5C, which is higher than that of other samples, and maintained 92.69% of its initial capacity at 5C after 100 cycles. Even at 10C after 100 cycles, it still had a capacity retention of 89.17%, demonstrating remarkable cycling stability.

Trial registration: ISRCTN NARL-D-17-00568

Keywords: Silver coating, $Li_4Ti_5O_{12}$/Ag, Lithium-ion batteries, Electrochemical performance

Highlights

1. Spherical $Li_4Ti_5O_{12}$/Ag composites were synthesized via a sol-gel-assisted hydrothermal method using ethylene glycol and a silver nitrate mixture as the precursor for the coating layer, which significantly improved the electronic conductivity and the electrochemical performance of $Li_4Ti_5O_{12}$.
2. The spherical morphology could induce a large tap density and consequently enhance the volumetric energy density.

Background

Over the last decade, rechargeable lithium-ion batteries (LIBs) have demonstrated many advantages. They are light weight; have a small size, high voltage and high energy density; and have been attracting intense interest as an electrochemical energy storage device to reduce exhaust emissions and for fuel economy [1, 2]. However, the price of lithium precursors, safety and life issues, and low power density are obstacles for the application of LIBs for large-scale energy storage in the future [3]. Therefore, to develop substitute materials to meet the demands of the safety of the large-scale storage, great efforts have been made [4].

Cube spinel lithium titanate ($Li_4Ti_5O_{12}$) materials, the anode materials of Li-ion batteries, have been become a promising material because of their zero-strain structural characteristic during the intercalation and deintercalation process of $Li_4Ti_5O_{12}$ [5–9]. This material has a platform lithium insertion and extraction voltage of ~ 1.55 V (vs. Li/Li^+), avoiding the formation of lithium-consuming solid electrolyte interface (SEI) films, which should be beneficial for enhancing safety and good cycling of the LIBs. Therefore, $Li_4Ti_5O_{12}$ has become one of the potential materials in commercial applications and scientific research. $Li_4Ti_5O_{12}$ has been prepared via various of methods, for example, solid-state, electroless deposition, microwave, and sol-gel method. Regarding the solid-state method,

* Correspondence: qhxylijun@gdut.edu.cn
Faculty of Chemical Engineering and Light Industry,, Guangdong University of Technology, No. 100 Waihuan xi Road, Guangzhou Higher Education Mega Center, Panyu District, Guangzhou, Guangdong 510006, China

some studies have shown that it has a simple synthesis route and low synthesis cost because of the shorter distance for Li^+ diffusion and electron transfer, $Li_4Ti_5O_{12}$ exhibits an excellent rate capability, but the solid-state reaction cannot provide a uniform morphology with a narrow size. However, the electroless deposition process has a complex synthesis route. For the sol-gel synthesis of $Li_4Ti_5O_{12}$, several researchers have reported that it can yield products with a uniformly homogeneous distribution and narrow particles with good stoichiometric control.

Despite these many advantages, the major drawbacks of $Li_4Ti_5O_{12}$ are its poor electronic and ionic conductivity and its slow Li-ion diffusion coefficient, which results in a poor rate capacity. Numerous strategies, including crystallite size reduction [10], doping with high valence metal ions [11–13], and coating with conducting phases [14–17], have been adopted to improve the discharge/charge transport properties of electrodes. In addition, another way to enhance the electronic conductivity is to synthesize nanostructured $Li_4Ti_5O_{12}$. The nanostructures provide a larger electrode/electrolyte contact area to increase the intercalation kinetics and reduce the diffusion paths to accelerate Li^+ and electron transport [18]. Among these approaches, the most effective way to improve the electrochemical properties of $Li_4Ti_5O_{12}$ is conductive surface modification. Aslihan et al. [2] synthesized $Li_4Ti_5O_{12}$ via the sol-gel method, and then the as-synthesized $Li_4Ti_5O_{12}$ was surface-coated with silver via electroless deposition. The results showed that silver coating (Ag coating) affords a highly conductive matrix for Li^+ insertion, improving the electronic conductivity. Zhu et al. [19] prepared carbon-coated nano-sized $Li_4Ti_5O_{12}$ nanoporous micro-spheres with a remarkable rate capability via a carbon pre-coating process in combination with a spray drying method, and indicated that the micron-sized spherical particles induce a large tap density, resulting in the enhancement of the volumetric energy density. However, how to synthesize Ag-coated micron-sized $Li_4Ti_5O_{12}$ spherical particles via a sol-gel-assisted hydrothermal method has not been reported.

Herein, we report a sol-gel-assisted hydrothermal method to synthesize the micron-sized spherical $Li_4Ti_5O_{12}$/Ag composite using ethylene glycol and a silver nitrate mixture as a precursor, and the content of the Ag coating was adjusted by controlling the amount of silver element in the precursor. The electrochemical properties of the $Li_4Ti_5O_{12}$/Ag with spherical morphology were investigated in detail.

Experimental

Synthesis of Pristine $Li_4Ti_5O_{12}$ and Modification of its Surface with Ag

Synthesis of the Spherical Precursor Via the Sol-Gel Method

The spherical precursor titanium glycolate (TG) was synthesized by the sol-gel method. First, 2 mL of tetrabutyl titanate was added slowly to the solution, which contained $AgNO_3$ (at an appropriate amount to be soluble in 50 mL of glycol), under vigorous stirring to form the precursor solution. Second, the precursor solution was added to a 150 mL of acetone mixture that contained 0.1 mL Tween 80, and agitation was continued for 1 h at room temperature to form precipitates. Then, the precipitates were aged for 8 h, separated by filtration, and washed twice with anhydrous alcohol. Finally, the precursor powders were obtained by heat treatment at 80 °C for 6 h in an oven followed by grinding.

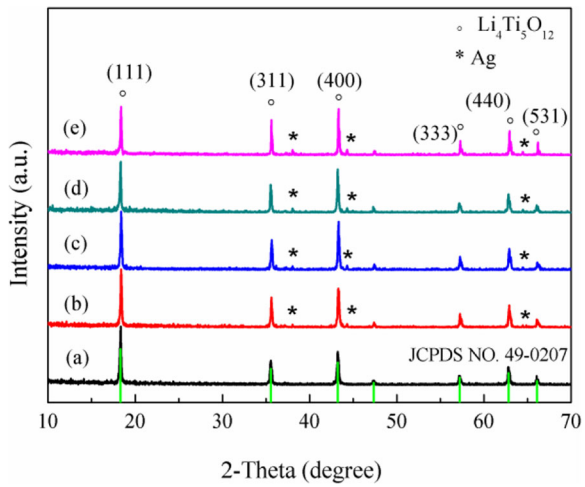

Fig. 1 XRD patterns of the $Li_4Ti_5O_{12}$/Ag. (**a**) 0 wt.%, (**b**) 1 wt.%, (**c**) 3 wt.%, (**d**) 5 wt.%, and (**e**) 7 wt.%

Synthesis of Spherical $Li_4Ti_5O_{12}$/Ag

The spherical $Li_4Ti_5O_{12}$/Ag was prepared via the hydrothermal method. First, $LiOH{\cdot}H_2O$ and the precursor in a molar ratio of 3.9:1 were homogeneously mixed by stirring with 40 mL of alcohol as the media for 1 h to form a mixture, which was then heated at 180 °C for 12 h in sealed Teflon wares until precipitates were obtained. Second, the precipitates were collected via centrifugation (5000 rpm, 5 min) and further washed with anhydrous ethanol several times. Then, they were dried in an oven at 80 °C for 2 h. Finally, the precipitates were heated in a muffle furnace at 700 °C for 2 h (heating rate of 5 $°C{\cdot}min^{-1}$) in air after they were

Table 1 Lattice parameters of the $Li_4Ti_5O_{12}$/Ag composites coated with different Ag contents

Content of Ag, wt.%	Lattice parameter (a = b = c), nm
0	0.83577
1	0.83572
3	0.83574
5	0.83576
7	0.83578

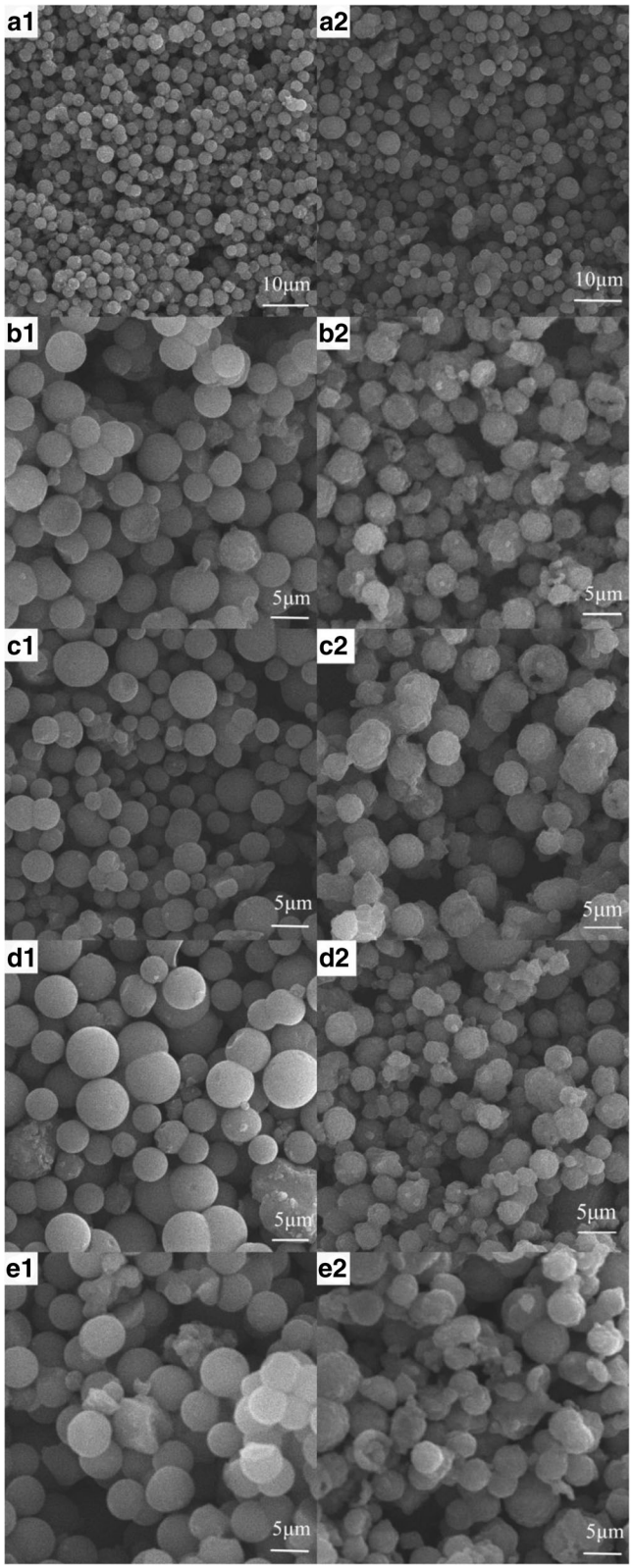

Fig. 2 SEM images of the precursor and the $Li_4Ti_5O_{12}$/Ag. (**a**) 0 wt.%, (**b**) 1 wt.%, (**c**) 3 wt.%, (**d**) 5 wt.%, (**e**) 7 wt.%

ground and then naturally cooled to room temperature to obtain spherical $Li_4Ti_5O_{12}$/Ag powder.

Material Characterization

The structure of the $Li_4Ti_5O_{12}$ samples were identified via X-ray diffraction (XRD, Rigaku D/max-PC2200) using a Cu Kα radiation (λ = 0.15405 nm) source with a scan rate of 4 °min^{-1} from 10° to 80° and operated at 40 KV and 20 mA. The morphology and particle size of the materials were explored via SEM (scanning electron microscopy, Supra 55 Zeiss) and TEM (transmission electron microscopy, JEOL-2100).

Electrochemical Measurements

The electrochemical performances of the products were tested using a CR2025 coin-type cell. The working electrodes were prepared by mixing 80 wt.% $Li_4Ti_5O_{12}$/Ag active materials, 10 wt.% conductive Super-P, and 10 wt.% polyvinylidene fluoride (PVDF) binder in N-methyl-2-pyrrolidone (NMP) solvent to form a uniform slurry. Then, the slurry was cast onto an aluminum foil and dried under vacuum at 80 °C for 12 h to remove the residual solvent. Then, the foil was pressed and cut into disks. A Celgard 2400 polypropylene microporous membrane and lithium foil were used as the separator and the negative electrode, respectively. The electrolyte solution was 1 M $LiPF_6$ in ethylene carbonate (EC), dimethyl carbonate (DMC), and ethylene methyl carbonate (EMC) in a volumetric ratio of 1:1:1. The cells were assembled in an argon-filled glove box, where both the moisture and oxygen levels were kept below 1 ppm. The electrochemical tests of the products were evaluated using a LAND CT2001A test system (Wuhan, China). Cyclic voltammetry (CV) tests were recorded on a CHI600A electrochemical workstation at a 0.1 mV s^{-1} scan rate from 1.0 to 2.5 V (vs. Li/ Li^+). EIS measurements were performed in the frequency range of 100 KHz to 10 mHz with a perturbation of 5 mV.

Results and Discussion

Structural and Morphological Properties

The effect of the amount of Ag additive on the $Li_4Ti_5O_{12}$/Ag powders was investigated. The XRD patterns of the Ag-coated spherical $Li_4Ti_5O_{12}$ composites are given in Fig. 1. It can be easily seen that the major diffraction peaks of all specimens appear at 18.4°, 35.54°, 43.2°, 57.2°, 62.8°, and 66.1° and are indexed as the (111), (311), (400), (333), (440), and (531), respectively. That peaks are in good agreement with the $Li_4Ti_5O_{12}$ standard diffraction pattern [20], except for characteristic patterns of the Ag metal (2θ = 38.1°, 44.3°, 64.4°). No impurity diffraction peaks were detected in any of the specimens. Moreover, the peak intensity of silver correspondingly increased as the amount of Ag increased.

Lattice parameters of the $Li_4Ti_5O_{12}$/Ag samples with different Ag coatings are provided in Table 1. No significant changes with the Ag content increase were observed. Thus, it was suggested that silver is mainly coating in the form of the elemental Ag on the surface of $Li_4Ti_5O_{12}$ particles but not penetrating into the lattice of spinel $Li_4Ti_5O_{12}$. Because the ionic radius of Ag^+ (0.126 nm) is substantially larger than that of the Ti^{4+} (0.068 nm), the as-synthesized $Li_4Ti_5O_{12}$/Ag sample was just a composite of the Ag metal and the $Li_4Ti_5O_{12}$ phase.

Figure 2 shows the SEM images of the as-prepared precursor (a_1-e_1) and $Li_4Ti_5O_{12}$/Ag (a_2-e_2). As shown in Fig. 2, all samples exhibit a uniformly spherical structure with a narrow size distribution of 5–10 μm, which is beneficial to a contact between the active materials and electrode. From the SEM images, the spherical precursor, titanium glycolate (TG) particles, shows a smooth line,

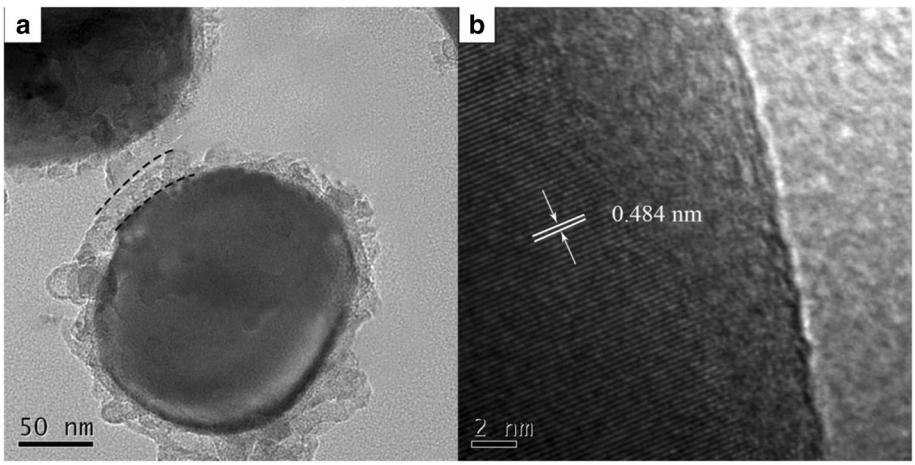

Fig. 3 (**a**) TEM and (**b**) HRTEM images of the 5 wt.% silver-coated $Li_4Ti_5O_{12}$, in which the "line" indicates the coated silver layer

whereas the $Li_4Ti_5O_{12}$/Ag particles presents a rough line. Moreover, a good dispersion could enlarge the electrode-electrolyte contact area and significantly accelerate the transportation of Li^+ and electron. However, the surface of the $Li_4Ti_5O_{12}$/Ag samples are not obviously smoother than that of the as-prepared precursor and titanium glycolate, and they exist to a certain extent as an agglomeration. Moreover, the particle sizes of different $Li_4Ti_5O_{12}$/Ag composites are much larger than that of Ag-free $Li_4Ti_5O_{12}$; however, the agglomeration phenomenon becomes more obvious with an increasing in silver content.

The distribution of silver in the interior of the micron-sized particles was further investigated, and TEM and HRTEM analyses were provided in Fig. 3. The TEM images (Fig. 3a) show that the 5 wt.% Ag-coated micron-sized-spherical $Li_4Ti_5O_{12}$ particles are uniformly coated by a silver layer with a thickness of 3~4 nm, indicating that the silver layer builds a conductive network on the surface of the entire material, which facilitates the lithium ion and electron transport. As shown in Fig. 3b, the surface of the micron-sized $Li_4Ti_5O_{12}$/Ag particles are not smooth, and the *d*-spacing of the 5 wt.% Ag-coated $Li_4Ti_5O_{12}$ particles is 0.484 nm, which matches well with that of the LTO (111) plane. This suggests that no new phase was generated on the surface of the LTO particles, but there was a thin coating layer on the particles.

Electrochemical Properties

Figure 4 shows the first charge-discharge curves of the micron-sized spherical $Li_4Ti_5O_{12}$/Ag electrodes coated

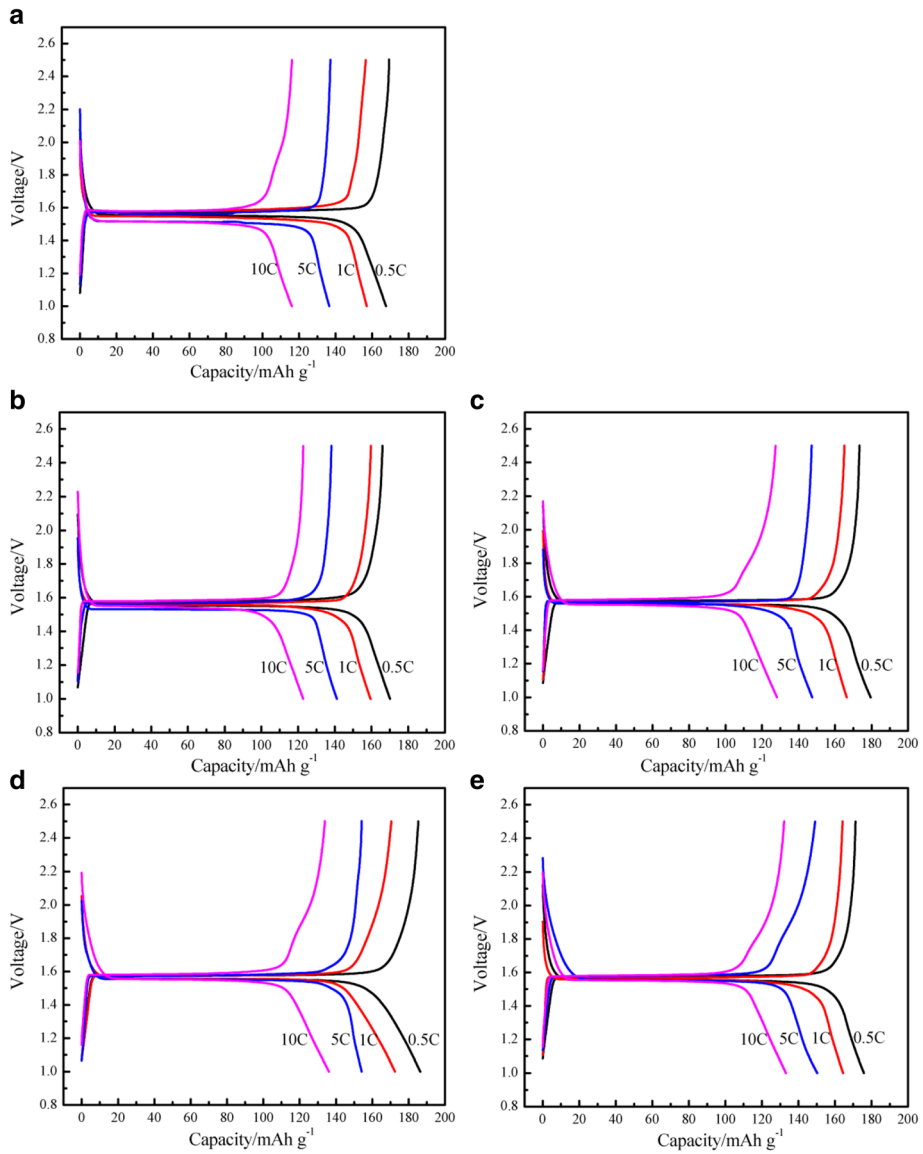

Fig. 4 The initial charge-discharge curves with various current densities of the $Li_4Ti_5O_{12}$/Ag. (**a**) 0 wt.%, (**b**) 1 wt.%, (**c**) 3 wt.%, (**d**) 5 wt.%, (**e**) 7 wt.%

with different Ag contents at the different rates. As it can be seen from Fig. 4, all of the profiles exhibit an extremely flat voltage plateau of 1.55 V (vs. Li/Li^+), indicating a two-phase transition between $Li_4Ti_5O_{12}$ and $Li_7Ti_5O_{12}$ for lithium insertion [21]. The voltage platform of $Li_4Ti_5O_{12}$/Ag composites is longer than that of Ag-free $Li_4Ti_5O_{12}$. With an increasing content of Ag, for a longer discharge platform of the $Li_4Ti_5O_{12}$/Ag composites, the ability to maintain the platform is stronger, suggesting that good electronic conductivity can effectively reduce the polarization of the material during the electrode reaction process, and improve the utilization of the material.

As shown in Fig. 4, Ag-free $Li_4Ti_5O_{12}$ delivered an initial discharge-specific capacity of 167.62 mAh g^{-1} at a rate of 0.5C, whereas the delivered capacity of the Ag-coated micron-sized spherical $Li_4Ti_5O_{12}$ composites increased with increasing silver amount: 170.10, 179.54, and 186.34 mAh g^{-1} for 1, 3, and 5 wt.%, respectively. But 7 wt.% Ag-coated $Li_4Ti_5O_{12}$ exhibited a somewhat different behavior. The delivered discharge-specific capacity decreased with increasing silver amount: 175.86 mAh g^{-1} for 7 wt.%. The 5 wt.% Ag-coated $Li_4Ti_5O_{12}$ gained the highest initial discharge capacity, and the initial discharge-specific capacities reached 186.34, 172.47, 154.12, and 136.06 mAh g^{-1} at the specific currents of 0.5, 1, 5, and 10C, respectively. Due to the poor electronic conductivity and sluggish Li^+ diffusion, the material exhibits a large polarization at high charge/discharge rates. The highly conductive Ag additive can significantly enhance the surface intercalation reaction and reduce the polarization [20, 22]. Even the highest Ag content (7 wt.%) can provide the longest voltage plateau, and the metal silver itself cannot be fully intercalated into the lithium. Instead, the high content of Ag will lead to a decrease in the specific capacity of $Li_4Ti_5O_{12}$/Ag. Therefore, an appropriate silver content can not only effectively improve the conductivity of the $Li_4Ti_5O_{12}$ and reduce the polarization of the $Li_4Ti_5O_{12}$ in the reaction process but can also reduce the loss of the reversible capacity due to the Ag coating.

The rate capabilities of the Ag-free $Li_4Ti_5O_{12}$ and 5 wt.% Ag-coated $Li_4Ti_5O_{12}$ composite were analyzed at current densities of 0.5, 1, 5, and 10C, and the results are shown in Fig. 5. As shown, the initial capacity of the 5 wt.% Ag-coated $Li_4Ti_5O_{12}$ composite at 5C was 154.12 mAh g^{-1}. After 30 cycles, the capacity was still maintained at 150.50 mAh g^{-1}, retaining over 97.65% of the initial capacity. When it was further increased to 10C, the discharge capacity apparently dropped from 136.06 mAh g^{-1} to 130.81 mAh g^{-1} after 30 cycles. While the retention efficiency of the capacity could still be maintained at 96.14%. What is more, the cycling performance of the $Li_4Ti_5O_{12}$/Ag composite was

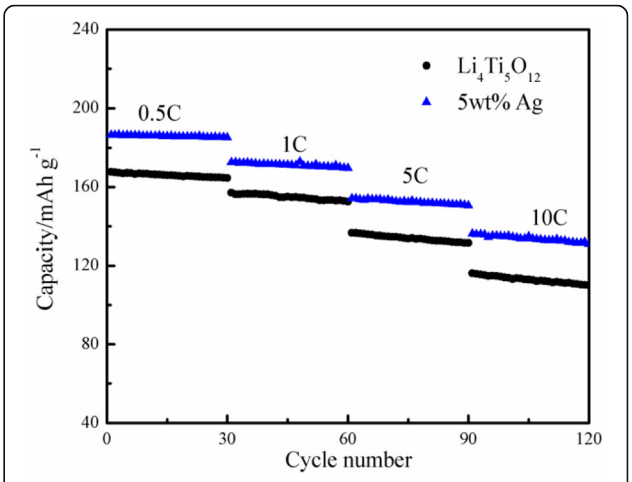

Fig. 5 Rate capability of the Ag-free and the 5 wt.% Ag-coated $Li_4Ti_5O_{12}$ under different current rates

significantly better than that of the Ag-free $Li_4Ti_5O_{12}$ at various charge-discharge rates. As shown in Fig. 6a, with an appropriate silver contents of 5 wt.%, the silver-coated $Li_4Ti_5O_{12}$ delivered the highest capacity of 186.34 mAh g^{-1} at 0.5C, which is higher than that of other samples, and maintained 92.69% of its initial capacity at 5C after 100 cycles. Even at 10C after 100 cycles (Fig. 6b), it still had a capacity retention of 89.17%, demonstrating remarkable cycling stability. The results suggested that under the favorable experimental conditions, the $Li_4Ti_5O_{12}$ surface Ag coating not only enhanced the electron and ionic conductivity but also obviously increased the electron transport during the lithium insertion/extraction reaction and significantly improved the cycle stability of the $Li_4Ti_5O_{12}$.

Figure 7 presents the cyclic voltammograms (CVs) of the Ag-free $Li_4Ti_5O_{12}$ and 5 wt.% Ag-coated $Li_4Ti_5O_{12}$ composite obtained at a slow rate of 0.1 mV s^{-1}. Obviously, reversible redox peaks between 1.0 and 2.5 V were obtained, which are attributed to the insertion and extraction of lithium ions, suggesting no intermediate phase formation during lithium insertion and de-insertion. Meanwhile, the redox peak area of these two curves is almost equal, indicating a high coulombic efficiency [23]. The potential differences between the oxidation and reduction peaks of the 5 wt.% Ag-coated $Li_4Ti_5O_{12}$ is 0.244 V, which is slightly lower than that of the Ag-free $Li_4Ti_5O_{12}$ (0.24 V). This suggests that appropriately surface coating the highly conductive Ag additive significantly reduced the polarization of the $Li_4Ti_5O_{12}$ sample and effectively improved its electrochemical performance. Moreover, the redox peaks of the 5 wt.% Ag-coated $Li_4Ti_5O_{12}$ are sharper and larger than that of Ag-free $Li_4Ti_5O_{12}$, which indicates that an appropriate Ag coating can improve the dynamic performance of the electrode.

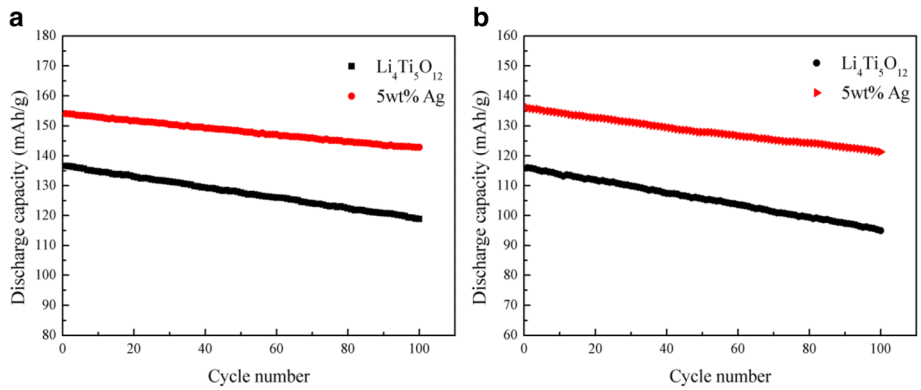

Fig. 6 The cycling performance of the Ag-free and the 5 wt.% Ag-coated $Li_4Ti_5O_{12}$ at 5 °C (**a**) and 10 °C (**b**)

Electrochemical impedance spectroscopy (EIS) measurements of Ag-free $Li_4Ti_5O_{12}$ and 5 wt.% Ag-coated $Li_4Ti_5O_{12}$ were conducted in the frequency range of 10^5 to 0.01 Hz before galvanostatic cycles. Additionally, the equivalent circuit (inset) and corresponding impedance data are shown in Fig. 8. In the equivalent circuit, *Rs* represents the electrolyte solution resistance, which reflects the electric conductivity of the electrolyte, separator, and electrodes. (intersection with the Z' axis at a high frequency), *R*ct shows the charge-transfer resistance in materials, *CPE* is the double-layer and passivation film capacitance, and *W* is the Warburg impedance, which is related to lithium ion diffusion in the low frequency region. The parameters obtained by fitting are listed in Table 2. As shown in Fig. 8, both EIS curves were composed of a depressed semicircle in the high-frequency region and an oblique straight line in the low-frequency region. The diameter of the semicircle stands for the charge-transfer resistance, and the oblique straight line is related to the Warburg impedance [24]. The impedance of the semicircles in the high frequency region correspond to the electrode and liquid electrolyte interface charge transfer process, and the straight line in the low frequency region can be expressed as the lithium ions' diffusion behavior in the oxide structure [25–28]. As shown from Fig. 8, the diameter of the semicircle of the 5 wt.% Ag-coated $Li_4Ti_5O_{12}$ is shorter than that of bare $Li_4Ti_5O_{12}$, indicating that a proper amount of Ag coating could enhance the electronic conductivity of $Li_4Ti_5O_{12}$, and this has to do with the charge-transfer process, where Li^+ and electrons reach the electrode surface simultaneously to complete the reaction. This mainly depends on the redox reaction across the surface of the active materials. The smaller charge-transfer resistance of the 5 wt.% Ag-coated $Li_4Ti_5O_{12}$ reflected a faster charge transfer reactions at their electrode/electrolyte interfaces.

The lithium ion chemical diffusion coefficient can be calculated from the plot in the low-frequency region by using the following Eq. (1) [29–33].

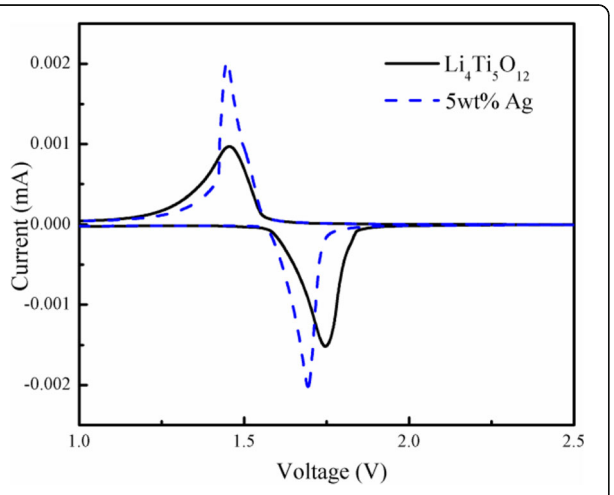

Fig. 7 CV curves of the Ag-free and the 5 wt.% Ag-coated $Li_4Ti_5O_{12}$ composite

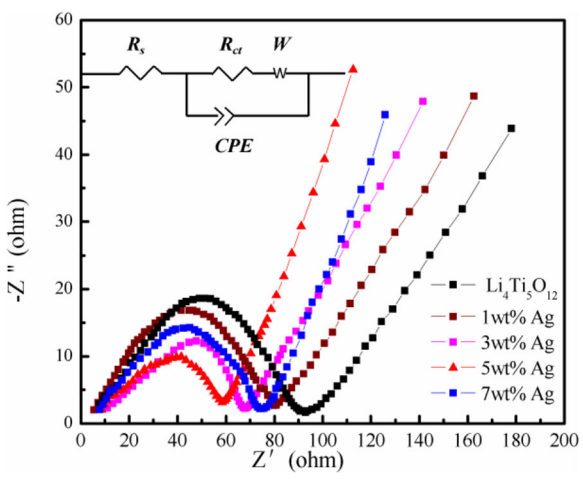

Fig. 8 EIS patterns of the pure $Li_4Ti_5O_{12}$ and the $Li_4Ti_5O_{12}$ coated with different Ag contents

Table 2 Impedance parameters of the pure $Li_4Ti_5O_{12}$ and the $Li_4Ti_5O_{12}$/Ag composites coated with different silver contents

Samples	Rs/Ω	Rct/Ω	$D_{Li}/cm^2\ s^{-1}$
$Li_4Ti_5O_{12}$	5.84	87.16	8.69×10^{-12}
$Li_4Ti_5O_{12}$/Ag (1 mass%)	4.56	77.44	2.14×10^{-11}
$Li_4Ti_5O_{12}$/Ag (3 mass%)	4.38	66.62	3.75×10^{-11}
$Li_4Ti_5O_{12}$/Ag (5 mass%)	4.13	57.87	6.73×10^{-11}
$Li_4Ti_5O_{12}$/Ag (7 mass%)	4.47	70.53	4.69×10^{-11}

$$D_{Li^+} = \frac{R^2T^2}{2A^2n^4F^4C_{Li}^2\sigma_w{}^2} \quad (1)$$

Here, D_{Li^+} is the lithium-ion diffusion coefficient, R is the gas constant (8.314 JK mol^{-1}), T is the absolute temperature (298 K), A is the surface area of the electrode, n is the number of electrons per molecule attending the electronic transfer reaction, F is the Faraday constant (96,500 C mol^{-1}), C_{Li} is the concentration of lithium ions in the $Li_4Ti_5O_{12}$ electrode, and σ_w is the Warburg factor, which has the following relationship with Z_{re}:

$$Z_{re} = R_S + R_{ct} + \sigma_w \cdot \omega^{-0.5} \quad (2)$$

Additionally, the relationship between Z_{re} and the reciprocal square root of frequency in the low frequency is shown in Fig. 9. All of the parameters obtained and calculated from the EIS are summarized in Table 2. As shown in Table 2, D_{Li^+} of the 5 wt.% Ag-coated $Li_4Ti_5O_{12}$ is 6.73×10^{-11}, which is one order of magnitude higher than that of $Li_4Ti_5O_{12}$ (8.69×10^{-12}). The 5 wt.% Ag-coated $Li_4Ti_5O_{12}$ has the largest lithium diffusion coefficient compared with that of Ag-free $Li_4Ti_5O_{12}$ and 1, 3, and 7 wt.% Ag-coated $Li_4Ti_5O_{12}$ composites, indicating that coating with Ag is an effective way to improve the electronic conductivity. Consequently, the rate capacity of the 5 wt.% Ag-coated $Li_4Ti_5O_{12}$ can be substantially improved.

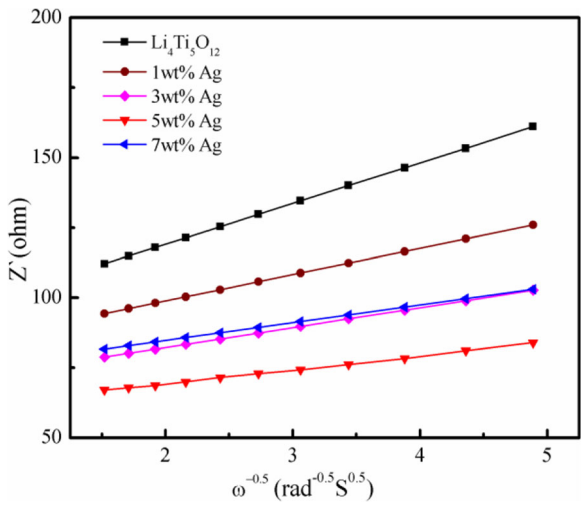

Fig. 9 Graph of Z_{re} plotted against $\omega^{-0.5}$ at the low frequency region for the $Li_4Ti_5O_{12}$ and $Li_4Ti_5O_{12}$ coated with different Ag contents

Conclusions

Anode materials spherical $Li_4Ti_5O_{12}$/Ag composites with a high tap density were prepared by a sol-gel-assisted hydrothermal method. The electrochemical tests show that the appropriate amount of Ag coating can significantly improve the electronic conductivity of $Li_4Ti_5O_{12}$ and enhance the cycle stability. The optimum content of silver is 5wt.%, which can get excellent electrochemical performance. However, the excessive silver content will cause the electrochemical properties of material worse. Therefore, appropriate Ag-coated spherical $Li_4Ti_5O_{12}$ composite is a superior lithium storage material with a high capacity and excellent safety, and it has real potential as a promising material in power lithium ion batteries.

Acknowledgements
This work is supported by Science and Technology Plan Foundation of Guangdong (2015A050502046) and Science and Technology Plan Foundation of Guangdong (201704030031).

Authors' Contributions
The idea is from JL, the manuscript was mainly written by SH and LL. The figures were mainly drawn by SX and LL and were calibrated by SL. All authors read and approved the final manuscript.

Ethics Approval and Consent to Participate
Not applicable.

Consent for Publication
Not applicable.

Competing Interests
The authors declare that they have no competing interests.

Publisher's Note

Received: 12 August 2017 Accepted: 13 October 2017
Published online: 30 October 2017

References

1. Wang Z, Liu E, Guo L, Shi C, He C, Li J, Zhao N (2013) Cycle performance improvement of Li-rich layered cathode material $Li[Li_{0.2}Mn_{0.54}Ni_{0.13}Co_{0.13}]O_2$ by ZrO_2 coating. Surf Coat Technol 235:570–576
2. Erdas A, Ozcan S, Nalci D, Guler MO, Akbulut H (2015) Novel Ag/$Li_4Ti_5O_{12}$ binary composite anode electrodes for high capacity Li-ion batteries. Surf Coat Technol 271:136–140
3. Chen C, Xu H, Zhou T, Guo Z, Chen L, Yan M, Mai L, Hu P, Cheng S, Huang Y, Xie J (2016) Integrated intercalation-based and interfacial sodium storage in graphene-wrapped porous $Li_4Ti_5O_{12}$ nanofibers composite aerogel. Adv Energy Mater 6:136–140
4. Chen C, Wen Y, Hu X, Ji X, Yan M, Mai L, Hu P, Shan B, Huang Y (2015) Na^+ intercalation pseudocapacitance in graphene-coupled titanium oxide enabling ultra-fast sodium storage and long-term cycling. Nat Commun 6:6929–6936

5. Ge H, Hao TT, Osgodd H, Zhang B, Chen L, Cui LX, Song XM, Ogoke O, Wu G (2016) Advanced mesoporous spinel $Li_4Ti_5O_{12}$/rGO composites with increased surface lithium storage capability for high-power lithium-ion batteries. ACS Appl Mater Interfaces 8:9162–9169
6. Bhatti HS, Anjum DH, Ullah S, Ahmed B, Habib A, Karim A, Hasanain SK (2016) Electrochemical characteristics and Li+ ion intercalation kinetics of Dual-Phase $Li_4Ti_5O_{12}/Li_2TiO_3$ composite in the voltage range 0–3 V. J Phys Chem C 120:9553–9561
7. Alaboina P, Ge Y, Uddin MJ, Liu Y, Lee D, Park S, Zhang XW (2016) Nanoscale porous lithium titanate anode for superior high temperature performance. ACS Appl Mater Interfaces 8:12127–12133
8. Mu DB, Chen YJ, Wu B, Huang R, Jiang Y, Li L, Wu F (2016) Nano-sized $Li_4Ti_5O_{12}$/C anode material with ultrafast charge/discharge capability for lithium ion batteries. J Alloys Compd 671:157–163
9. Long DH, Jeong MG, Lee YS, Choi W, Lee JK, Oh IH, Jung HG (2015) Coating Lithium Titanate with nitrogendoped carbon by simple refluxing for high-power lithium-ion batteries. ACS Appl Mater Interfaces 7:10250–10257
10. Kavan L, Prochazka J, Spitler TM, Kalbac M, Zukalova MT, Drezen T, Gratzel M (2003) Li Insertion into $Li_4Ti_5O_{12}$ (spinel) charge capability vs. particle size in thin-film electrodes. J Electrochem Soc 150:A1000–A1007
11. Chen CH, Vaughey JT, Jansen AN, Dees DW, Kahaian AJ, Goacher T, Thackeray MM (2001) Studies of Mg–substituted $Li_{4-x}Mg_xTi_5O_{12}$ spinel electrodes ($0 \leq x \leq 1$) for lithium batteries. J Electrochem Soc 148:A102–A104
12. Wolfenstine J, Allen JL (2008) Electrical conductivity and charge compensation in Ta doped $Li_4Ti_5O_{12}$. J Power Sources 180:582–585
13. Cheng Q, Tang S, Liu C, Qian L, Zhao J, Liang J, Yan J, Liu Z, Cao Y-C (2017) Preparation and electrochemical performance of $Li_{4-x}Mg_xTi_5O_{12}$ as anode materials for lithium-ion battery. J Alloys Compd 722:229–234
14. Park KS, Benayad A, Kang DJ, Doo SG (2008) Nitridation-driven conductive $Li_4Ti_5O_{12}$ for lithium ion batteries. J Am Chem Soc 130:14930–14931
15. Wang YQ, Guo L, Guo YG, Li H, He XQ, Tsukimoto S, Ikuhara Y, Wan LJ (2012) Rutile-TiO_2 nanocoating for a high-rate $Li_4Ti_5O_{12}$ anode of a lithium-ion battery. J Am Chem Soc 134:7874–7879
16. Jung H, Myung S, Yoon CS, Son S, Oh KH, Amine K, Scrosati B, Sun Y (2011) Microscale spherical carbon-coated $Li_4Ti_5O_{12}$ as ultra high power anode material for lithium batteries. Energy Environ Sci 4:1345–1351
17. Cheng Q, Tang S, Liu C, Qian L, Zhao J, Liang J, Wei F, Liu Z-Q, Cao Y-C Preparation of carbon encapsulated $Li_4Ti_5O_{12}$ anode material for lithium ion battery through pre-coating method. Ionics. https://doi.org/10.1007/s11581-017-2093-y
18. Liu D, Cao G (2010) Engineering nanostructured electrodes and fabrication of film electrodes for efficient lithium ion intercalation. Energy Environ Sci 3:1218–1237
19. Zhu G, Liu H, Zhuang J, Wang C, Wang Y, Xia Y (2011) Carbon-coated nano-sized $Li_4Ti_5O_{12}$ nanoporous-microsphere as anode material for high-rate lithium-ion batteries. Energy Environ Sci 4:4016–4022
20. Huang SH, Wen ZY, Zhu XJ, Gu ZH (2004) Preparation and electrochemical performance of Ag doped $Li_4Ti_5O_{12}$. Electrochem Commun 6:1093–1097
21. Lan C-K, Bao Q, Huang Y-H, Duh J-G (2016) Embedding nano-$Li_4Ti_5O_{12}$ in hierarchical porous carbon matrixes derived from water soluble polymers for ultra-fast lithium ion batteries anodic materials. J Alloys Compd 673:336–348
22. Huang SH, Wen ZY, Yang XJ, Gu ZH, Xu XH (2005) Improvement of the high-rate discharge properties of $LiCoO_2$ with the Ag additives. J Power Sources 148:72–77
23. Li J, Huang S, Li SF, Xu SJ, Pan CY (2017) Synthesis and electrochemical performance of $Li_4Ti_5O_{12}$/Ag composite prepared by electroless plating. Ceram Int 43:1650–1656
24. Zhu W, Yang H, Zhang W, Huang H, Tao X, Xia Y, Gan Y, Guo X (2015) Synthesis and electrochemical performance of $Li_4Ti_5O_{12}$/C nanocrystallines for high-rate lithium ion batteries. RSC Adv 5:74774–74782
25. Wu FX, Li XH, Wang ZX, Guo HJ, Wu L, Xiong XH, Wang XJ (2011) Preparation of TiO_2 nanosheets and $Li_4Ti_5O_{12}$ anode material from natural ilmenite. Powder Technol 213:192–198
26. Li J, Jin YL, Zhang XG, Yang H (2007) Microwave solid-state synthesis of spinel $Li_4Ti_5O_{12}$ nanocrystallites as anode material for lithium-ion batteries. Solid State Ionics 178:1590–1597
27. Wan ZN, Cai R, Jiang SM, Shao ZP (2012) Nitrogen- and TiN-modified $Li_4Ti_5O_{12}$: one-step synthesis and electrochemical performance optimization. J Mater Chem 22:17773–17781
28. Shenouda AY, Murali KR (2008) Electrochemical properties of doped lithium titanate compounds and their performance in lithium rechargeable batteries. J Power Sources 176:332–339
29. Yi T-F, Fang Z-K, Deng L, Wang L, Xie Y, Zhu Y-R, Yao J-H, Dai C (2015) Enhanced electrochemical performance of a novel $Li_4Ti_5O_{12}$ composite as anode material for lithium-ion battery in a broad voltage window. Ceram Int 41:2336–2341
30. Yi T-F, Yang S-Y, Tao M, Xie Y, Zhu Y-R, Zhu R-S (2014) Synthesis and application of a novel $Li_4Ti_5O_{12}$ composite as anode material with enhanced fast charge-discharge performance for lithium-ion battery. Electrochim Acta 134:377–383
31. Yi T-F, Yang S-Y, Zhu Y-R, Ye M-F, Xie Y, Zhu R-S (2014) Enhanced rate performance of $Li_4Ti_5O_{12}$ anode material by ethanol-assisted hydrothermal synthesis for lithium-ion battery. Ceram Int 40:9853–9858
32. Liu W, Shao D, Luo G, Gao Q, Yan G, He J, Chen D, Yu X, Fang Y (2014) Enhanced rate performance of $Li_4Ti_5O_{12}$ anode material by ethanol-assisted hydrothermal synthesis for lithium-ion battery. Electrochim Acta 133:578–582
33. Yi T-F, Chen B, Shen H-Y, Zhu R-S, Zhou A-N, Qiao H-B (2013) Spinel Li4Ti5-xZrxO12 ($0 \leqslant x \leqslant 0.25$) materials as high-performance anode materials for lithium-ion batteries. J Alloy Compd 558:11–17